Advances in Complex Systems Vol. 22, Nos. 7 & 8 (2019) 1950023 (19 pages) © World Scientific Publishing Company DOI: 10.1142/S0219525919500231



THE ACTUATION SPECTRUM OF SPATIOTEMPORAL NETWORKS WITH POWER-LAW TIME DEPENDENCIES

QI CAO*

 $\label{eq:continuous} Department of Industrial and Systems Engineering, \\ Rensselaer Polytechnic Institute, \\ Troy, NY \\ caoq2@rpi.edu$

GUILHERME RAMOS

Institute for Systems and Robotics,
Instituto Superior Técnico, Universidade de Lisboa,
Lisbon, Portugal
guilherme.ramos@tecnico.ulisboa.pt

PAUL BOGDAN

 $\begin{tabular}{ll} \it Ming Hsieh Department of Electrical Engineering, \\ \it University of Southern California, \\ \it Los Angeles, CA \\ \it pbogdan@usc.edu \end{tabular}$

SÉRGIO PEQUITO

 $\label{eq:continuity} Department of Industrial and Systems Engineering, \\ Rensselaer Polytechnic Institute, \\ Troy, NY \\ goncas@rpi.edu$

Received 30 June 2019 Revised 8 January 2020 Accepted 30 January 2020 Published 11 March 2020

The ability to steer the state of a dynamical network towards a desired state within a time horizon is intrinsically dependent on the number of driven nodes considered, as well as the network's topology. The trade-off between time-to-control and the minimum number of driven nodes is captured by the notion of the actuation spectrum (AS). We study the actuation spectra of a variety of artificial and real-world networked systems, modeled by fractional-order dynamics that are capable of capturing non-Markovian time properties with power-law dependencies. We find evidence that, in both types of networks, the actuation spectra are similar when the time-to-control is less or equal to about 1/5 of the size of the network. Nonetheless, for a time-to-control larger than the network size, the minimum number of driven nodes required to attain controllability in networks with fractional-order dynamics may still decrease in

^{*}Corresponding author.

comparison with other networks with Markovian properties. These differences suggest that the minimum number of driven nodes can be used to determine the true dynamical nature of the network. Furthermore, such differences also suggest that new generative models are required to reproduce the actuation spectra of real fractional-order dynamical networks.

Keywords: Complex networks; control theory; fractional calculus and dynamical systems; network controllability; minimum number of driven nodes.

1. Introduction

Assuring that the state of a dynamical system can be steered from a given or arbitrary initial state into a desired final one in finite time is one of the fundamental problems studied in the control theory [12, 17, 19]. This property is captured by the notion of *controllability* and is of paramount importance in a variety of applications, such as in chemical process control, multi-agent networks, large-scale flexible structures, systems biology, and power systems [13, 34, 35].

In the recent decades, much work has been devoted to developing tools to analyze and design networked dynamical systems with regards to their controllability or related properties [8, 25, 28, 30]. The problem of identifying a minimal subset of driving or driven nodes in order to ensure the controllability of a system has proved to be computationally intractable, and, even for the simpler scenario of the linear time-invariant (LTI) systems, NP-hard [23, 30, 31]. Notwithstanding, some characterization on the minimum number of driving nodes (i.e., the number of inputs with a possibly large number of state nodes receiving the input) are available and polynomially computable [40, 43, 44]. Scientific advances in this front combine efforts from fields such as control theory, network science, and statistical physics [19]. The concepts of controllability and controllability subspaces (and their reachability counterparts) [12, 17] allow us to assign meaning to the ability of steering a set of state nodes in a networked dynamical system into a desired state by means of external input. In what follows, we will consider driven nodes that correspond to a state node that is actuated by a single driving node, which only actuates that state node [23, 30, 31].

A common assumption in state-space models of the dynamical systems is the absence of (temporal) memory, often referred to as *Markovian* time dependencies. However, this is in striking contrast with several biological systems whose dynamics do exhibit memory characteristics, including long-term memory dependencies. For instance, certain parameters or measurements of physiological activity, as well as other applications like viscoelastic [4], electric circuits [42] and biological conductance [1], possess non-Markovian time dependencies, in the form of the aforementioned long-term memory [21, 36, 37, 39]. Furthermore, their dynamics can often be well represented via spatiotemporal models with power-law decaying memory [11, 15, 16, 38].

A particular class of such power-law memory decay models is the class of fractional-order dynamical systems, in which derivatives or difference operators

appear in non-integer orders on state-space representations. Indeed, unlike the classical integer-order derivatives or difference operators, fractional-order ones, which are the main object of study in the mathematical field of the *fractional calculus* [5, 14, 32, 33], act non-locally on the functions that they are applied to. This way, they induce long-term memory when the fractional-order derivative of a state vector is set as a function of itself [9, 18, 22, 24].

A substantial portion of the paradigms to study controllability properties focuses solely on whether or not the state of a system can be driven into a desired one, independently of the required time needed to attain it [19, 23, 27]. To address this situation, the *controllability index* [12] was proposed, which measures the smallest interval of time needed to drive the state into a desired one. Later, in [29], the concept of *it is actuation spectrum* (AS) was introduced, which encapsulates the trade-offs between the minimum number of driven nodes and the controllability indices.

Furthermore, we would like to clarify that our research focuses on understanding the trade-offs between the system parameters (in particular, long-term or long-range memory (dependence)) and the time-to-control, as well as the minimum number of driven nodes required. Another dimension would be to also consider the energy budget allowed to control fractional-order systems. Note that to some extent, our version is tied with energy budget in the sense that as we allow more time for the system to be controlled, less energy would be required as the controllability Gramian is monotonically decreasing with the time horizon [10].

The authors observed that in most complex networks, whether artificial or real, only a small fraction of driven nodes is needed to control the network within a relatively small window of time. Furthermore, for networked systems with uncertain parameters (i.e., weights), the authors explored the AS regarding *structural controllability* (also called *network controllability*) and observed that, for artificial network models generated in order to mimic certain structural properties of the real-world networks, their actuation spectrum were often substantially different than those of their real-world network counterparts.

In this paper, we investigate the AS in the context of networked systems modeled by (discrete-time) fractional-order linear dynamics. We note that, compared to a Markovian system, introducing memory could help in reducing the smallest number of driven nodes required to control a networked system due to the possible synergistic effects of the memory regarding external inputs. On the other hand, memory could also, in theory, result in needing a larger number of driven nodes, since the synergistic effect of the memory could prove counter-productive regarding the controllability of the system.

In this work, we propose to provide an answer to the aforementioned conundrum, by studying the actuation spectrum of several artificial fractional-order linear dynamical networks (FODN), and real-world ones as identified using techniques such as described in [15]. We noticed that in both types of networks, the actuation spectra are similar when the time-to-control is less or equal to about 1/5 of the size of the network. Nonetheless, the minimum number of driven nodes needed to reach the

controllability in networks with fractional-order dynamics appears to be smaller for a time-to-control larger than the network size for networks with a known non-Markovian nature. These differences indicate that the minimum number of driven nodes can be used to determine the true dynamical nature of the network. Besides, such differences also suggest that new generative models are required to reproduce the actuation spectrum of real fractional-order dynamical networks.

2. Methodology

We will first review some important concepts regarding linear fractional-order systems, we will formally define the AS, and we will state the problem being addressed. Then we will succinctly derive a necessary and sufficient condition for controllability, and introduce a greedy approximation algorithm to solve the problem.

2.1. Problem statement

Suppose that the dynamics of a networked system can be modeled as a discrete-time FODN, whose dynamics can be described as follows:

$$\Delta^{\alpha} x[k+1] = A(\mathcal{G})x[k] + Bu[k], \quad x[0] = x_0 \quad (k=0,1,2,\ldots),$$
 (1)

where $x[k] \in \mathbb{R}^n$ denotes the stacked states of the network with n nodes at time step $k, u[k] \in \mathbb{R}^p$ denotes the stacked external input signals driving the states of the network at time $k, A(\mathcal{G})$ denotes an adjacency matrix that describes the spatial dependencies upon the topology of the underlying network graph \mathcal{G} , in which an entry is zero if there is no connection between two nodes, and B is the input matrix that describes how the input signal is distributed across different states. Additionally, $\boldsymbol{\alpha} = (\alpha_1, \dots, \alpha_n)$ and $\Delta^{\alpha} = \operatorname{diag}(\Delta^{\alpha_1}, \dots, \Delta^{\alpha_n})$, where Δ^{α_i} denotes the Grünwald–Letnikov fractional-order difference operator of order $\alpha_i \in \mathbb{R} \setminus \{-1, -2, \dots\}$ (usually positive numbers, referred to as coefficients or exponents), given by

$$\Delta^{\alpha_i} x_i [k+1] \triangleq \sum_{j=0}^{k+1} (-1)^j {\alpha_i \choose j} x_i [k-j], \tag{2}$$

for $i=1,\ldots,n$, where $\binom{\alpha_i}{j} \triangleq \frac{\Gamma(\alpha_i+1)}{\Gamma(j+1)\Gamma(\alpha_i-j+1)}$ generalizes the usual binomial coefficient $\frac{\alpha_i!}{j!(\alpha_i-j)!}$ for $\alpha_i \in \mathbb{Z}_+$ through the Gamma function $\Gamma(z) \triangleq \int_0^\infty t^{z-1}e^{-t}dt$, defined for $z \in \mathbb{C} \setminus \{-1,-2,\ldots\}$, which satisfies $\Gamma(z+1) = z!$ for $z \in \mathbb{Z}_+$. For simplicity, we refer to the system in (1) by the triple $\mathcal{F}(A(\mathcal{G}); B; \boldsymbol{\alpha})$.

Furthermore, in order to control the FODN, we need to provide a certain number of external input nodes to control state variables in a finite number of steps. In what follows, we are particularly interested in the driven nodes with dedicated driving nodes obtained by designing the input matrix to be of the form $B = \mathbb{I}_n^{\mathcal{J}}$, where $\mathcal{J} \subseteq \{1, \ldots, n\}$ denotes the indices of the actuated state nodes, and

$$\begin{bmatrix} \mathbb{I}_n^{\mathcal{J}} \end{bmatrix}_{ij} \triangleq \begin{cases} 1, & \text{if } i = j \in \mathcal{J}, \\ 0, & \text{otherwise.} \end{cases}$$
(3)

The FODN described by $\mathcal{F}(A(\mathcal{G}), B; \boldsymbol{\alpha})$ is controllable in K steps if and only if, for every initial state $x_0 \in \mathbb{R}^n$ and desired final state $x_{\text{des}} \in \mathbb{R}^n$, there exists a sequence $u[0], \ldots, u[K-1]$ of inputs such that $x[0] = x_0$ and $x[K] = x_{\text{des}}$. Consequently, there is an implicit trade-off between the minimum number of driven nodes and the time-to-control K. Following [29], the AS for a FODN can be defined as a function $s: \mathbb{N} \to \{1, \ldots, n\}$ given by

$$s(K) \triangleq \min_{\mathcal{J} \subseteq \{1, \dots, n\}} |\mathcal{J}|$$

s.t. $\mathcal{F}(A(\mathcal{G}), \mathbb{I}_n^{\mathcal{J}}; \boldsymbol{\alpha})$ is controllable in K steps. (\mathcal{P})

In other words, s(K) denotes the minimum number of driven nodes required to control the network such that the resulting FODN is controllable in K steps. Note that for LTI systems, s(K) = s(n) for every $K \geq n$, as a consequence of invoking the Cayley–Hamilton theorem in deriving the controllability matrix for the LTI systems. However, this may not be true for FODNs due to their long-term memory, and, in particular, due to their associated controllability matrices, over which the Cayley–Hamilton theorem cannot be employed, given that such controllability matrices are not based on powers of any given matrix.

In this paper, the objective is to study the actuation spectrum for FODNs, in order to understand in what way they are affected by the non-Markovian nature of FODNs, in particular, to understand if fewer or more input nodes are needed when long-term memory is introduced in an otherwise LTI system.

2.2. Greedy approximation algorithm

In the following paragraphs, we will revisit the controllability properties for FODN and explain how to approximately obtain the minimum number of driven nodes needed to control $\mathcal{F}(A(\mathcal{G}), B; \boldsymbol{\alpha})$ within K steps. It is worth noticing that, unfortunately, (\mathcal{P}) can be proved to be NP-hard by invoking the duality between controllability and observability for a given K (see [41]). Therefore, we will build our results upon the work in [41] to approximately calculate the actuation spectrum of FODNs in polynomial time, by providing suboptimal solutions to Problem (\mathcal{P}) with optimality guarantees.

First, note that the state vector x[k] in (1) can be expressed as

$$x[k] = G_k x[0] + \sum_{j=0}^{k-1} G_{k-1-j} Bu[j], \tag{4}$$

where G_k is recursively defined as

$$G_k = \left\{ \begin{array}{ll} \mathbb{I}_n & \text{for } k=0, \\ \displaystyle \sum_{j=0}^{k-1} A_j G_{k-1-j} & \text{for } k \geq 1, \end{array} \right.$$

Q. Cao et al.

with $A_0 = A(\mathcal{G}) - \operatorname{diag}(\alpha_1, \dots, \alpha_n)$ and

$$A_{j} = \begin{bmatrix} (-1)^{j} {\alpha_{1} \choose j+1} & & & \\ & \ddots & & \\ & & (-1)^{j} {\alpha_{n} \choose j+1} \end{bmatrix},$$
 (5)

for $j \neq 0$. Therefore, for $x[0] = x_0$, we have

$$x[k] = G_k x_0 + \underbrace{\left[G_0 B \dots G_{k-1} B\right]}_{\mathcal{C}_k} \begin{bmatrix} u[k-1] \\ \vdots \\ u[0] \end{bmatrix}, \tag{6}$$

where C_k denotes the (k-step) controllability matrix. Therefore, $\mathcal{F}(A(\mathcal{G}), B; \boldsymbol{\alpha})$ is controllable in K steps if and only if $rank(\mathcal{C}_K) = n$. Indeed, in that case, we may choose

$$\begin{bmatrix} u[K-1] \\ \vdots \\ u[0] \end{bmatrix} = \mathcal{C}_K^{\top} (\mathcal{C}_K \mathcal{C}_K^{\top})^{-1} (x_{\text{des}} - G_K x_0), \tag{7}$$

which will lead to $x[K] = x_{\text{des}}$ when starting from $x[0] = x_0$.

Note that the control law is, in fact, similar to the one employed in the LTI scenario, but it contrasts with the LTI case, where if it is controllable it has to be in at most n time steps, and for FODN, it is theoretically possible to attain rank equal to n for K > n.

Algorithm 1. Greedy Algorithm to approximately solve (\mathcal{P})

```
input: A, \alpha, K;
```

output: \mathcal{J}^* that is an approximate solution to (\mathcal{P}) ;

- 1: $\mathcal{J}^{\star} \leftarrow \emptyset$;
- 2: go to step 4
- 3: while $\Delta r^{\star} > 0$ do
- $j^{\star} \leftarrow \operatorname{argmax}_{j \in \{1, \dots, n\}} \operatorname{rank}(\mathcal{C}_{K}(\mathcal{J}^{\star} \cup \{j\}));$ $\Delta r^{\star} \leftarrow \operatorname{rank}(\mathcal{C}_{K}(\mathcal{J}^{\star} \cup \{j^{\star}\})) \operatorname{rank}(\mathcal{C}_{K}(\mathcal{J}^{\star}));$
- if $\Delta r^{\star} > 0$ then 6:
- $\mathcal{J}^{\star} \leftarrow \mathcal{J}^{\star} \cup \{j^{\star}\};$ 7:
- end if
- 9: end while

Towards obtaining the minimum number of driven nodes to achieve controllability of a FODN within K time-steps, it is possible to show that the set function $f(\mathcal{J}) \triangleq \operatorname{rank}(\mathcal{C}_K(\mathcal{J}))$ is submodular [41], where $\mathcal{C}_K(\mathcal{J})$ denotes the K-step controllability matrix of system $\mathcal{F}(A(\mathcal{G}), \mathbb{I}_n^{\mathcal{I}}; \boldsymbol{\alpha})$. Subsequently, we can employ a greedy approximation algorithm, described in Algorithm 1, to approximately solve (\mathcal{P}) , whose output is at most 33% worse than an exact solution (and it is noted in several applications to have tight experimental bounds [3, 20]) and has computational complexity $\mathcal{O}(n^5)$ [42].

3. Results

In what follows, we obtain the actuation spectrum for the different FODNs. Specifically, we consider both artificial FODNs (Sec. 3.1) and real-world networked systems modeled as FODNs (Sec. 3.2). To assess the actuation spectrum of artificial networks, we consider three of the most common models: (i) Erdös–Rényi (ER), (ii) Barabási–Albert (BA), and (iii) Watts–Strogatz (WS). Within each model, we consider multiple realizations with specific fixed fractional exponents, as well as exponents uniformly sampled from the open unit interval. Next, we consider real-world data in the form of four multivariate time series produced by the neurophysiological networked systems modeled as either an LTI system or an FODN.

3.1. Actuation spectrum for artificial FODNs

In this section, we studied the AS for artificial FODNs. We considered three undirected and unweighted network models whose adjacency matrices define the state transition matrices of the corresponding systems: (i) Erdős-Rényi (ER), which is perhaps the simplest random network model; (ii) Barabási-Albert (BA), which produces scale-free networks; and (iii) WS, which produces small-world networks. Each of the network models was generated with n = 50 nodes and only considered if fully connected. For each network model, we generated 100 network realizations in order to later compute the average values and variances of the actuation spectra. The actuation spectra for the ER, BA, and WS are presented in Figs. 1-3, respectively. Each figure depicts different parametric choices for each row, where in the first column we display a particular realization of the corresponding network model. In the second column, we computed, for different (but fixed) fractional coefficients $\alpha \in \{0.1, 0.5, 0.8, 1\}$, the average of the actuation spectra for each of the 100 generated networks. Finally, in the third column, we generated 30 values of α from the uniform distribution $\mathcal{U}(0,1)$ and computed the actuation spectrum for all combinations of parameters and α , followed by computing the average in α for each of the 100 networks, and finally the average of those 100 approximated spectra was computed, as well as their corresponding standard deviations.

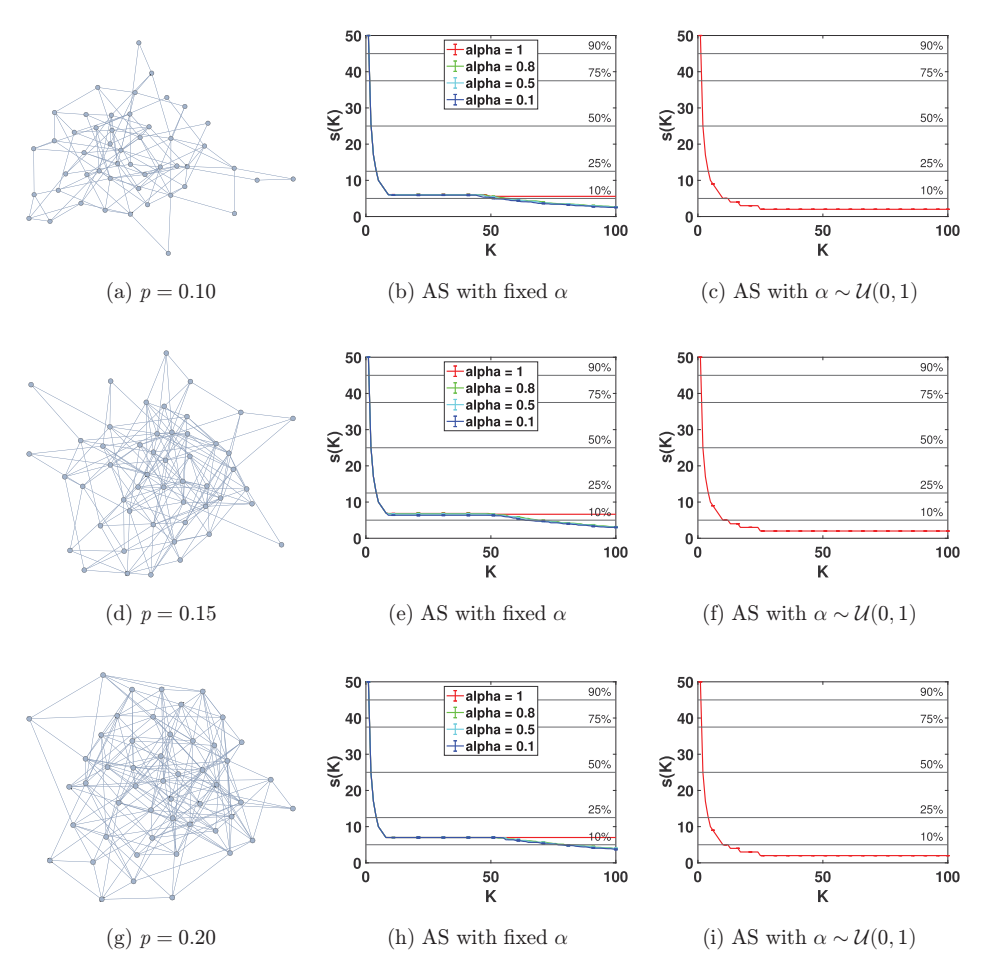


Fig. 1. ER network model with n=50 nodes and probability $p \in \{0.10, 0.15, 0.20\}$ of establishing a new edge between two nodes during construction.

3.1.1. Erdös–Rényi (ER) network model

The results for three ER network models with n=50 nodes are displayed in Fig. 1, where the probability p of linking any two pairs of nodes in the construction of the networks is chosen as $p \in \{0.10, 0.15, 0.20\}$. The actuation spectrum for the different parametric choices of p are provided in the second column, where the fractional coefficients are assumed fixed, while in the third column, the average actuation spectra are depicted where the coefficients are independently sampled from a uniform distribution $\mathcal{U}(0,1)$.

From the results displayed in Fig. 1, we obtain evidence that seems to indicate that there are no major differences in the actuation spectra, other than appearing to decrease slightly faster with smaller p. Furthermore, we can see that the minimum

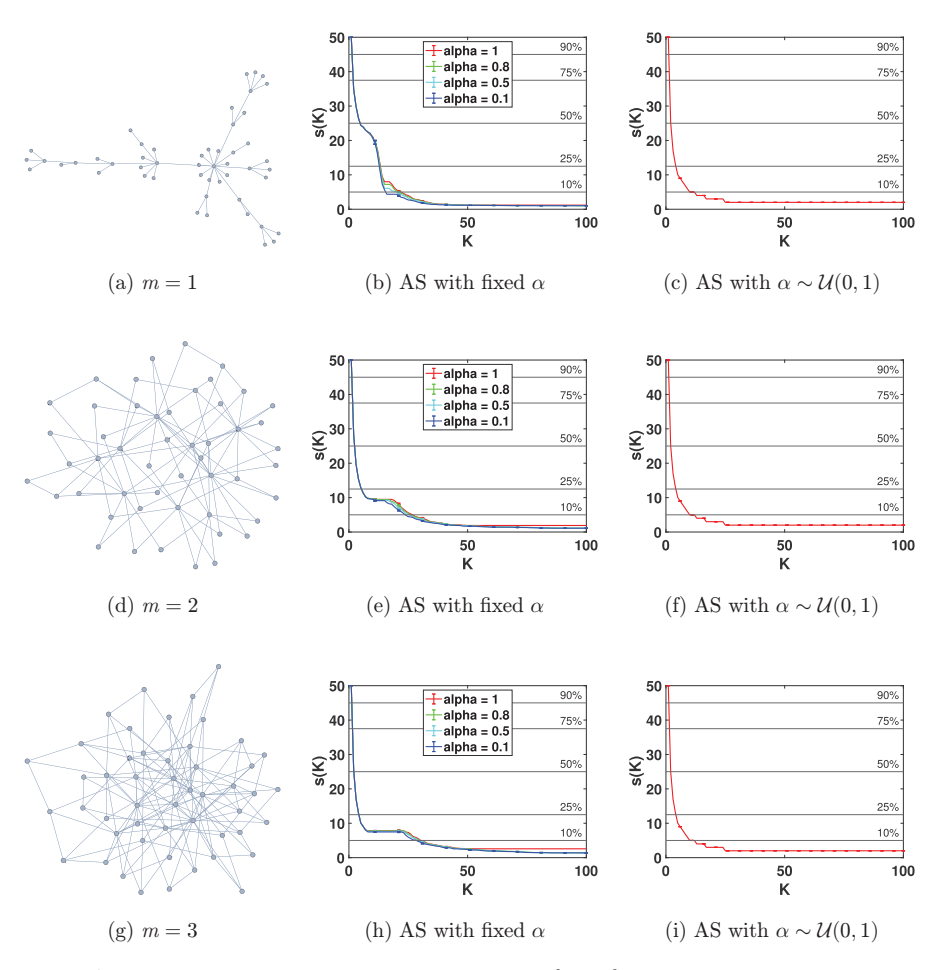
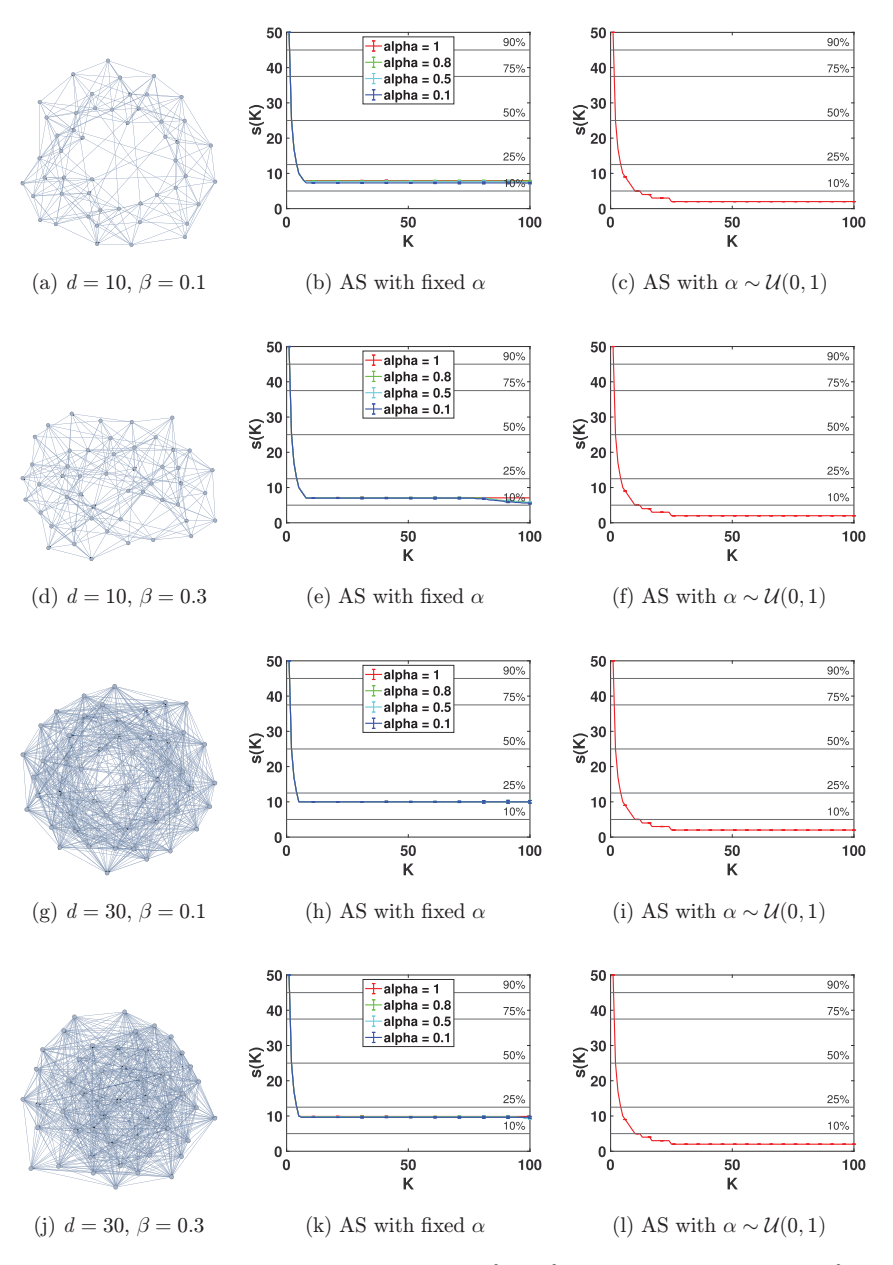


Fig. 2. BA network model with n=50 nodes and $m\in\{1,2,3\}$ new connections per iteration of construction.

number of driven nodes steeply decreases as the control horizon K increases, reaching less than 10% of the nodes before K=10. The decrease in the minimum number of driven nodes became much slower thereafter. In addition, from the actuation spectra plots of the ER model, we also see that it does not significantly depend on p or α , provided the connectedness of the network holds. In practice, connectedness is not strictly required, for we can typically focus on the controllability of subsystems, for instance those defined by the connected components of the network [44]. To further strengthen the latter observation, in the third column of Fig. 1, we show the averaged actuation spectra for randomly chosen values of the fractional coefficients α in (0,1). The shapes of the curves in these actuation spectra plots are similar to the shapes of curves in the spectra plots with fixed α , which once again suggests that the exponent $\alpha \in (0,1)$ does not have strong effects on the number of driven nodes required to control the ER model network.

$Q.\ Cao\ et\ al.$



 $\text{Fig. 3.} \quad \text{WS network model with } n=50 \text{ nodes, degree } d \in \{10,30\}, \text{and rewiring probability } \beta \in \{0.1,0.3\}.$

3.1.2. Barabási–Albert (BA) network model

The results for three BA network models are displayed in Fig. 2, where the number m of edges needed to attach at every step of construction is chosen as $m \in \{1, 2, 3\}$. The second column of Fig. 2 shows the AS, for each of the three considered BA network

models when the fractional coefficient is considered fixed but different. The actuation spectra appear to indicate that as m changes, there are significant differences in the minimum number of inputs to achieve smaller values of K. Specifically, the larger the value m, the larger (i.e., larger K) we can control the network with only 10% of the driven nodes. Nonetheless, it seems that the behavior is the opposite for smaller values of K when more than 10% of driven nodes are required. For instance, if we want to control the network in K=10, then the smaller m leads to a higher minimum number of driven nodes. It is also remarkable to notice that when less than 10% of the driven nodes are required, there is a slow decay in the minimum number of driven nodes, but such decay seems more pronounced for lower values of m. Further, we have also considered the case where the different networks possess fractional coefficients that are chosen at random between zero and one, whose results are displayed in the third column of Fig. 2. These results provide evidence that different levels of temporal memory (encapsulated in the fractional coefficients) do not seem to affect the AS across the different BA FODN.

3.1.3. Watts-Strogatz (WS) network model

The AS for the WS network model is displayed in Fig. 3 when the neighboring degrees are d=10 and d=30, and the rewiring probabilities are $\beta=10\%$ and $\beta = 30\%$. The second column of Fig. 3 shows the actuation spectra of the corresponding network models for different but fixed fractional coefficients $\alpha \in \{0.1, 0.5, 0.8, 1\}$. The results obtained suggest that there is a faster decay when the degree d increases until only 1/5 of the driven nodes are required. In particular, with 1/5 of the state nodes being driven, we are able to attain controllability for K=5 when the degree is d=30, and K=8 when d=10. Additionally, it seems that the regularity of the FODN for lower degrees (i.e., d=10) and higher re-wiring probability (i.e., $\beta = 0.30$) leads to a smaller number of driven nodes required to attain controllability after larger values of K (i.e., K > 70). However, when the degree increases (i.e., when d=30), the behavior becames similar. Another interesting observation is that the minimum number of driven nodes seems to be approximately constant after K=25 when the fractional coefficients are selected uniformly at random between zero and one for the lower degree and re-wiring probability, as well as the higher degree and re-wiring probability; and leading to lower s(K) than the fixed fractional coefficients in the remaining cases.

3.2. Actuation spectrum of real-world FODNs

We studied the actuation spectrum of four different neurophysiological networks, in which data are collected in the form of multivariate time series to be soon described. In order to model their dynamics, both LTI systems and FODNs will be considered, and their corresponding actuation spectra provided. Additionally, the differences obtained between LTI and FODN models will be captured by the distribution of the

Q. Cao et al.

entry-wise absolute differences between the matrices capturing the interdependencies between the state variables, as well as the fractional coefficients for the FODN (as these are all equal to one in the LTI case). All the results are summarized in Fig. 4, where by row we have the data for the different networks, and by columns (from left to right) the samples of the time series obtained from different networks, modeling statistics (i.e., the distributions of the absolute differences entry-wise and fractional coefficients), and AS. Next, we describe in more detail the datasets considered from which real networks were constructed.

3.2.1. Functional magnetic resonance imaging (fMRI) in resting state

This dataset consists of n=32 state variables encoded as the nodes corresponding to brain volumes captured by the functional magnetic resonance imaging (fMRI) in the

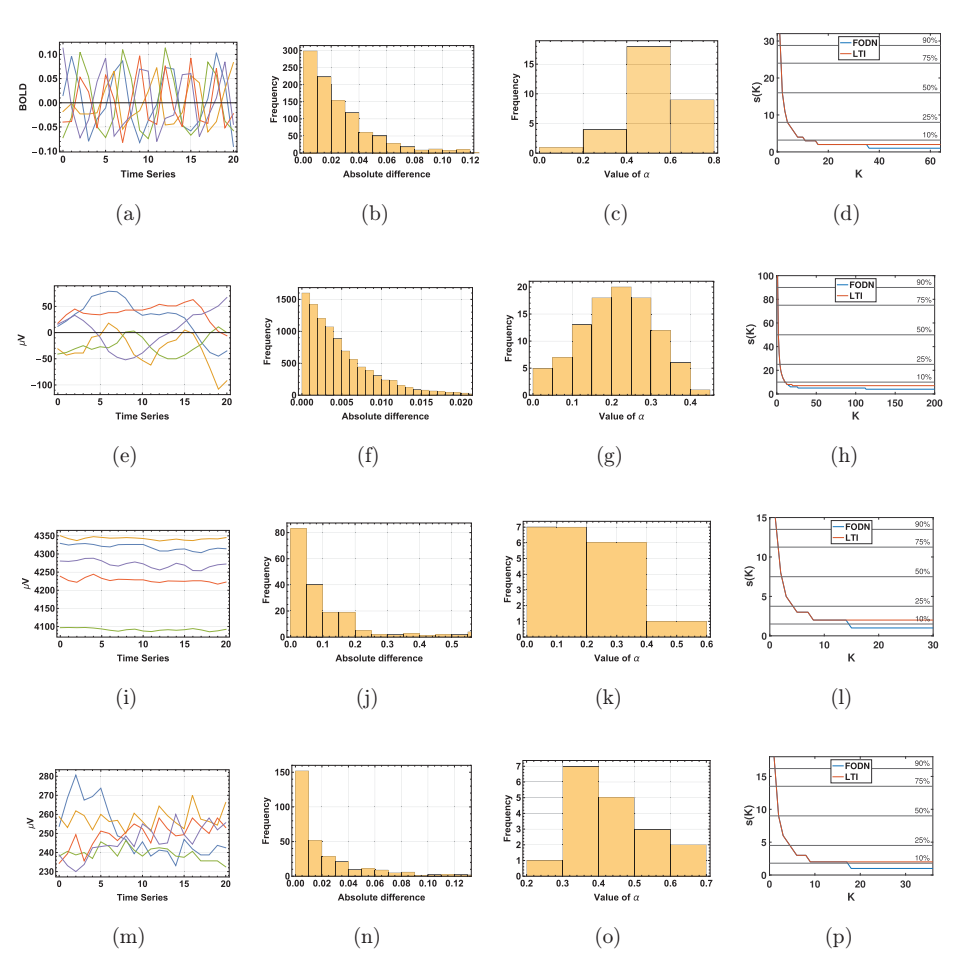


Fig. 4. Results for real-world networks modeled from neurophysiological datasets.

so-called resting state [7], where blood-oxygen-level-dependent (BOLD) imaging signals are tracked to form a multivariate time series. An excerpt of the time series is depicted in Fig. 4(a). The original dataset contains a total of 1200 subjects, of which 1113 had 3T MR scans. We have randomly chosen one of these subjects and computed the actuation spectrum when LTI and FODN models are fitted to the corresponding time series (see [15]). In order to understand the differences in the models obtained, in Fig. 4(b), we present the distribution of the absolute difference entrywise between the states' interdependency matrices $A(\mathcal{G})$ obtained for the LTI and FODN. Additionally, whereas the LTI corresponds to the particular case of FODN where all fractional coefficients are equal to one, we can see in Fig. 4(c) that different state variables in the FODN model have different fractional coefficients. The actuation spectrum for the two different models are shown in Fig. 4(d). The actuation spectrum for the LTI and FODN models exhibit similar behavior until K=36, and it seems that the minimum number of driven nodes becomes constant starting at K=16 for the LTI model. Notwithstanding, for K>36 the minimum number of driven nodes is smaller in the case of FODN in comparison with the LTI model.

3.2.2. Skull-level electroencephalographic (EEG) data in resting state

This dataset consists of n = 100 nodes corresponding to single-channel electroencephalographic (EEG) segments. Time series were collected from the different nodes during a 23.6 s time window, generated from skull-level (i.e., surface) EEG recordings one out of five healthy volunteers (dataset A in [2]) relaxed in an awake state with eyes open (i.e., resting state). An excerpt of the time series formed by the data is shown in Fig. 4(e). Both LTI and FODN models were considered to describe the time series of the EEG recordings. The modeling differences shown in Fig. 4(f) present the distribution of the absolute difference entrywise between the states' interdependency matrices $A(\mathcal{G})$ obtained for the LTI and FODN. In Fig. 4(g), we see that for the FODN, different state variables have different exponents. The actuation spectrum of the two different models are present in Fig. 4(h), where we can see that the two actuation spectra coincide until K=15, after which the minimum number of driven nodes to attain controllability is smaller in the FODN. Furthermore, it is interesting to remark that the minimum number of driven nodes to attain controllability remains constant after K = 17 in the LTI, but continues to decrease in FODN until K = 113, being constant afterwards with 4 fewer driven nodes than in the LTI.

3.2.3. Electroencephalographic (EEG) data for open-closed eyes

This dataset consists of n=14 nodes corresponding to 14 EEG channels recorded using the skull-level Emotiv EEG Neuroheadset, where electrical potentials are measured, and time series. An excerpt of the time series is depicted in Fig. 4(i). The data used was selected from an EEG eye state dataset, where during a 117s time

 $^{^{\}rm a}$ https://datahub.io/machine-learning/eeg-eye-state\#data.

window, the eyes alternate between open and closed. In the dataset, '1' denotes the eye-close state and '0' represents the eye-open state. In Fig. 4(j), we present the distribution of the absolute difference entrywise between the states' interdependency matrices $A(\mathcal{G})$ obtained for the LTI and FODN models. In Fig. 4(k), we notice that different state variables have different fractional coefficients when the network is modeled as a FODN. The actuation spectrum of the two different models are present in Fig. 4(l), where we can see that they overlap until K=13 and the LTI stabilizes after K=7, after which a smaller minimum number of driven nodes is required to attain controllability in the FODN. Also, notice that the minimum number of driven nodes to attain controllability decreases from K=13 to K=15, and remains equal to one afterward.

3.2.4. Electromyographic (EMG) data

This dataset consists of n=18 stave variables associated with nodes corresponding to the electromyographic (EMG) data signals generated from a clinical experiment [42], which compared muscle contractions of trans-radial amputees to those of nonamputated subjects. Electrical potential variations are collected at the muscle level in the forearm to form a multivariate time series, which is exemplified in Fig. 4(m). In Fig. 4(n), we present the distribution of the absolute difference entrywise between the states' interdependency matrices $A(\mathcal{G})$ obtained for the LTI and FODN. The fractional coefficients of the FODN are displayed in Fig. 4(o). The actuation spectra of the two models are present in Fig. 4(p), from which we can see that they overlap until K=17, the LTI stabilizes after K=9, and the FODN stabilizes after K=19. The minimum number of driven nodes required to attain controllability in the FODN is smaller for K>17, and remains equal to one afterward.

4. Discussion

4.1. Actuation spectrum of artificial networks

It is remarkable to notice that the results obtained seem to indicate that there are both similarities and striking differences on the AS across different models and parameters therein. Specifically, both the LTI-based and the FODN models seem to exhibit a rapid decay in the required minimum number of driven nodes to attain controllability for a time-to-control (i.e., K) approximately equal to 1/5 of the network size. Most FODN models and parameters also seem to allow for a fewer number of driven nodes to attain controllability for times-to-control larger than the size of the network.

Intriguingly, there are some important exceptions. For instance, the WS networks display a complex relationship among the control requirements (i.e., the minimum number of driven nodes and time-to-control), the degree of heterogeneity in the fractional coefficients, the neighboring degrees and the re-wiring probabilities. More

precisely, the non-Markovian WS networks with heterogeneous fractional coefficients across states (associated with all the nodes in the network), require a minimum number of driven nodes to attain controllability for times-to-control larger than the size of the network that matches the requirements of LTI (Markovian) WS networks. These observations open the door to better understand the controllability of the brain, as neural activity exhibits complex small-world properties [6]. In particular, it might allow us to combine regulation on the fractional coefficients and a smaller number of driven nodes to attain controllability of the brain.

Lastly, and consistently with the results reported about the actuation spectra of LTI [29], the transient from time-to-control equal to 1/5 of the network to the size of the network exhibits different behaviors across the different network models. Specifically, there are different transients (i.e., decays) across the different network modes, where the fastest seems to be the WS, followed by the ER, and lastly the BA. Nonetheless, it is interesting to remark that while the transient is almost indistinguishable between LTI and FODN in the WS and ER models, there are some differences in the BA model. Specifically, during the transient between time-to-control equal to 1/5 to the size of the network, the lower the fractional coefficient, the smaller the minimum number of driven nodes required to attain controllability.

4.2. On the actuation spectrum of real networks

The actuation spectra in real networks seems to indicate that there are indeed differences in the minimum number of driven nodes required to attain controllability when the time-to-control becomes near or greater the size of the network. Such findings are particularly important since they provide us with a mechanism to validate the true nature of the real networks (i.e., are then LTI or FODN). Specifically, we can envision experiments where we consider the minimum number of driven nodes to attain a time-to-control larger than the size of the network and inject the control signals in the real network according to the control laws previously described. If we can steer the real network towards an arbitrary desirable state with the control laws of an FODN, then it cannot be modeled as an LTI as it would require a larger number of driven nodes to achieve an arbitrary desirable goal.

Another intriguing observation is that there are some real networks where the actuation spectra of the LTI and FODN becomes distinct for a considerable small time-to-control (e.g., the skull-level EEG data in the resting-state network). Specifically, a smaller number of driven nodes to attain controllability of the FODN is required starting at a time-to-control equal to 13. This would allow us to control the network faster, but, most remarkably, it also brings up the point that the AS is different from those observed across the different artificial networks. Therefore, the present results provide further evidence and in line with [18] that we need to create new models that are able to capture the diverse transients in the actuation spectra of real networks not captured by most common artificial network models.

4.3. Computation of the actuation spectrum

It is worth noticing that computing the exact actuation spectra is a computational challenge for a variety of reasons. First, the computation of a rank of a large matrix leads to numerical instability issues that are only aggravated by taking the rank of its powers. Ultimately, the numerical instability is associated with the conditioning number of the matrices $A(\mathcal{G})$ considered to represent the different networks. As such, in order to mitigate the effect of such numerical issues, we kept the dimension of the networks manageable and performed the computations with high-computational precision, with further validation on the exact rank obtained.

Secondly, as mentioned in the Methodology section, the problem of determining the minimum number of inputs is NP-hard. Therefore, only approximation schemes can be considered to achieve the results in a reasonable amount of time. Fortunately, the objective functions considered satisfying the so-called *submodularity* property may be often found in different applications, and the submodular functions enable the use of greedy algorithms that provide a certificate of sub-optimality guarantees (i.e., at most 33% worse than the optimal), for which several studies report that in fact, the results obtained are near optimal [3, 20]. Ultimately, the small variation observed when performing several experiments to obtain the different actuation spectra for the artificial networks also indicates that we are indeed near optimal as we get approximately the same minimum number of driven nodes across similar networks as acknowledged in the literature [29].

It is also important to note that the actuation spectra can also be approximated by considering network controllability properties (i.e., using structural systems theory) [29]. In fact, determining the minimum number of driven nodes using this framework has been done under the restrictive assumption that all parameters (i.e., the fractional coefficients and states interdependency matrices) are independent of each other across different times [26]. Consequently, this would prevent us to assess the real effect of memory in the controllability properties of FODN, which leads us to the framework considered in this paper.

Acknowledgments

Q.C. and S.P. gratefully acknowledges the support by the National Science Foundation under the CMMI-1936578.

P.B. acknowledges support by the National Science Foundation under the Career Award CPS/CNS-1453860, CCF-1837131, MCB-1936775, CNS-1932620, CMMI-1936624, Defense Advanced Research Projects Agency (DARPA) Young Faculty Award under grant number N66001-17-1-4044. The views, opinions, and/or findings contained in this article are those of the author and should not be interpreted as representing the official views or policies, either expressed or implied by the Defense Advanced Research Projects Agency, the Department of Defense or the National Science Foundation.

G.R. is with the Institute for Systems and Robotics, Instituto Superior Técnico, Universidade de Lisboa, Lisboa, Portugal. He acknowledges the support of Institute for Systems and Robotics, Instituto Superior Técnico (Portugal), through scholarship BL112/2019_IST-ID. This work was partially supported by the Portuguese Fundação para a Ciência e a Tecnologia (FCT) through Institute for Systems and Robotics (ISR), under Laboratory for Robotics and Engineering Systems (LARSyS) project UID/EEA/50009/2019.

References

- Anastasio, T. J., The fractional-order dynamics of brainstem vestibulo-oculomotor neurons, Biol. Cybernet. 72 (1994) 69-79.
- [2] Andrzejak, R. G., Lehnertz, K., Mormann, F., Rieke, C., David, P. and Elger, C. E., Indications of nonlinear deterministic and finite-dimensional structures in time series of brain electrical activity: Dependence on recording region and brain state, *Phys. Rev. E* 64 (2001) 061907.
- Bach, F. et al., Learning with submodular functions: A convex optimization perspective, Found. Trends[®] Mach. Learn. 6 (2013) 145–373.
- [4] Bagley, R. L. and Torvik, P., A theoretical basis for the application of fractional calculus to viscoelasticity, J. Rheol. 27 (1983) 201–210.
- [5] Baleanu, D., Machado, J. A. T. and Luo, A. C., Fractional Dynamics and Control (Springer Science & Business Media, 2011).
- [6] Bassett, D. S. and Bullmore, E., Small-world brain networks, Neuroscientist 12 (2006) 512–523.
- [7] Becker, C. O., Pequito, S., Pappas, G. J., Miller, M. B., Grafton, S. T., Bassett, D. S. and Preciado, V. M., Spectral mapping of brain functional connectivity from diffusion imaging, Sci. Rep. 8 (2018) 1411.
- [8] Becker, C. O., Pequito, S., Pappas, G. J. and Preciado, V. M., Network design for controllability metrics, in 2017 IEEE 56th Annual Conf. Decision and Control (CDC) (IEEE, 2017), pp. 4193–4198.
- [9] Box, G. E., Jenkins, G. M., Reinsel, G. C. and Ljung, G. M., Time Series Analysis: Forecasting and Control (John Wiley & Sons, 2015).
- [10] Boyd, S. and Lall, S., EE263: Introduction to linear dynamical systems, Online Lecture Notes, Stanford University (2008).
- [11] Chatterjee, S., Romero, O. and Pequito, S., A separation principle for discrete-time fractional-order dynamical systems and its implications to closed-loop neurotechnology, *IEEE Control Syst. Lett.* **3** (2019) 691–696.
- [12] Chen, C.-T., Linear System Theory and Design (Oxford University Press, Inc., 1998).
- [13] Egerstedt, M., Complex networks: Degrees of control, Nature 473 (2011) 158–159.
- [14] Gorenflo, R. and Mainardi, F., Fractional calculus, in Fractals and Fractional Calculus in Continuum Mechanics (Springer, 1997), pp. 223–276.
- [15] Gupta, G., Pequito, S. and Bogdan, P., Dealing with unknown unknowns: Identification and selection of minimal sensing for fractional dynamics with unknown inputs, in *Proc.* 2018 American Control Conf. (IEEE, 2018), pp. 2814–2820.
- [16] Gupta, G., Pequito, S. and Bogdan, P., Learning latent fractional dynamics with unknown unknowns, in Proc. 2019 American Control Conf. (IEEE, 2019), pp. 217–222.
- [17] Hespanha, J. P., Linear Systems Theory (Princeton University Press, 2018).

- [18] Klamka, J., Controllability and minimum energy control of fractional discrete-time systems, in Controllability and Minimum Energy Control (Springer, 2019), pp. 89–98.
- [19] Liu, Y.-Y. and Barabási, A.-L., Control principles of complex systems, Rev. Mod. Phys. 88 (2016) 035006.
- [20] Lovász, L., Submodular functions and convexity, in Mathematical Programming The State of the Art (Springer, 1983), pp. 235–257.
- [21] Lundstrom, B. N., Higgs, M. H., Spain, W. J. and Fairhall, A. L., Fractional differentiation by neocortical pyramidal neurons, *Nat. Neurosci.* 11 (2008) 1335.
- [22] Machado, J., Discrete-time fractional-order controllers, Fract. Calc. Appl. Anal. 4 (2001) 47–66.
- [23] Olshevsky, A., Minimal controllability problems, IEEE Trans. Control Netw. Syst. 1 (2014) 249–258.
- [24] Ortigueira, M. D., Coito, F. J. and Trujillo, J. J., Discrete-time differential systems, Signal Process. 107 (2015) 198–217.
- [25] Pasqualetti, F., Zampieri, S. and Bullo, F., Controllability metrics, limitations and algorithms for complex networks, *IEEE Trans. Control Netw. Syst.* 1 (2014) 40–52.
- [26] Pequito, S., Bogdan, P. and Pappas, G. J., Minimum number of probes for brain dynamics observability, in 2015 54th IEEE Conf. Decision and Control (CDC) (IEEE, 2015), pp. 306–311.
- [27] Pequito, S., Kar, S. and Aguiar, A. P., A framework for structural input/output and control configuration selection in large-scale systems, *IEEE Trans. Autom. Control* 61 (2015) 303–318.
- [28] Pequito, S., Preciado, V. and Pappas, G. J., Distributed leader selection, in 2015 54th IEEE Conf. Decision and Control (CDC) (IEEE, 2015), pp. 962–967.
- [29] Pequito, S., Preciado, V. M., Barabási, A.-L. and Pappas, G. J., Trade-offs between driving nodes and time-to-control in complex networks, Sci. Rep. 7 (2017) 39978.
- [30] Pequito, S., Ramos, G., Kar, S., Aguiar, A. P. and Ramos, J., The robust minimal controllability problem, Automatica 82 (2017) 261–268.
- [31] Ramos, G., Pequito, S. and Caleiro, C., The robust minimal controllability problem for switched linear continuous-time systems, in 2018 Annual American Control Conf. (ACC) (IEEE, 2018), pp. 210–215.
- [32] Rudolf, H., Applications of Fractional Calculus in Physics (World Scientific, 2000).
- [33] Sabatier, J., Agrawal, O. P. and Machado, J. T., Advances in Fractional Calculus, Vol. 4 (Springer, 2007).
- [34] Siljak, D., Large-Scale Dynamic Systems: Stability and Structure, Dover Civil and Mechanical Engineering Series (Dover Publications, 2007).
- [35] Skogestad, S., Control structure design for complete chemical plants, Comput. Chem. Eng. 28 (2004) 219–234.
- [36] Thurner, S., Windischberger, C., Moser, E., Walla, P. and Barth, M., Scaling laws and persistence in human brain activity, Phys. A. Stat. Mech. Appl. 326 (2003) 511–521.
- [37] Turcott, R. G. and Teich, M. C., Fractal character of the electrocardiogram: Distinguishing heart-failure and normal patients, Ann. Biomed. Eng. 24 (1996) 269–293.
- [38] Tzoumas, V., Xue, Y., Pequito, S., Bogdan, P. and Pappas, G. J., Selecting sensors in biological fractional-order systems, *IEEE Trans. Control Netw. Syst.* 5 (2018) 709–721.
- [39] Werner, G., Fractals in the nervous system: Conceptual implications for theoretical neuroscience, Front. Physiol. 1 (2010) 15.
- [40] Wonham, W. M., Linear multivariable control, in Optimal Control Theory and its Applications (Springer, 1974), pp. 392–424.

- [41] Xue, Y., Pequito, S., Coelho, J. R., Bogdan, P. and Pappas, G. J., Minimum number of sensors to ensure observability of physiological systems: A case study, in 2016 54th Annual Allerton Conf. Communication, Control, and Computing (Allerton) (IEEE, 2016), pp. 1181–1188.
- [42] Yang, X.-J., Machado, J. T., Cattani, C. and Gao, F., On a fractal lc-electric circuit modeled by local fractional calculus, *Commun. Nonlinear Sci. Numer. Simul.* 47 (2017) 200–206.
- [43] Zhou, T., Minimal inputs/outputs for a networked system, IEEE Control Syst. Lett. 1 (2017) 298–303.
- [44] Zhou, T., Minimal inputs/outputs for subsystems in a networked system, Autom. 94 (2018) 161–169.